Advanced Pharmacokinetic Models Based on Organ Clearance, Circulatory, and Fractal Concepts

Submitted: January 29, 2007; Accepted: May 14, 2007; Published: June 29, 2007

K. Sandy Pang,[1] Michael Weiss,[2] and Panos Macheras[3]

[1]Leslie Dan Faculty of Pharmacy, University of Toronto, 144 College Street, Toronto, Ontario, Canada M5S 3M2
[2]Section of Pharmacokinetics, Department of Pharmacology, Martin Luther University Halle-Wittenberg, 06097 Halle, Germany
[3]Laboratory of Biopharmaceutics- Pharmacokinetics, Faculty of Pharmacy, University of Athens, Athens, Greece

Abstract

Three advanced models of pharmacokinetics are described. In the first class are physiologically based pharmacokinetic models based on in vitro data on transport and metabolism. The information is translated as transporter and enzyme activities and their attendant heterogeneities into liver and intestine models. Second are circulatory models based on transit time distribution and plasma concentration time curves. The third are fractal models for nonhomogeneous systems and non-Fickian processes are presented. The usefulness of these pharmacokinetic models, with examples, is compared.

Keywords: Pharmacokinetic models, physiologically based pharmacokinetic, PBPK, models, liver, kidney, circulatory models, distribution, fractal models, homogeneous, nonhomogeneous

Introduction

One of the most important outcomes in pharmacokinetic modeling is the ability to predict drug levels and/or dynamic behaviors of drug entities in the body. Another is the deduction of mechanistic insight into what events have happened. Sometimes the question is not how realistic the models are but what is their consistency and adequacy in making predictions. Most models are oversimplifications of the reality, but we have to start somewhere. It is certainly the hopes of pharmacokineticists that the models are easy to assemble, useful, and relevant.

Various approaches have emerged to predict blood/plasma and tissue concentration time profiles and/or provide mechanistic insight into what events have occurred. Compartmental approaches are the simplest and most widely used. The premise is based on venous equilibration and mass transfer into and out of compartments. In recent decades, however, modeling techniques have become more sophisticated. There is the departure from the compartmental modeling approach to physiological modeling in order to confer more significance to the anatomy, flow, and discrete eliminatory and/or distributional organs in the body.[1] Among these more advanced models, 3 forms are described in this mini-review. First are the zonal and segmental physiologically based pharmacokinetic (PBPK) liver and intestinal models. Second is the circulatory model that can account for concentration differences within the vascular space or sampling compartment. Third is the fractal model that is relevant to systems with smaller dimensions, namely, fractal spaces or disordered systems. In this communication, we present the bases behind the models and the kind of information one can extract from them.

Corresponding Author: K. Sandy Pang, Leslie Dan Faculty of Pharmacy, University of Toronto, 144 College Street, Toronto, Ontario, Canada M5S 3M2. Tel: 416-978-6164; Fax: 416-978-8511; E-mail: ks.pang@utoronto.ca

Physiologically Based Pharmacokinetic Organ Models

Physiologically Based Pharmacokinetic Model for Organs

The physiologically based pharmacokinetic (PBPK) model is the simplest starting point in physiological modeling that relates organ or tissue structures to the physiology of the organ or tissue, and is based on the concept that compartments are homogeneous and well-stirred (Figure 1).[2] Each organ or tissue of discrete volume is perfused by blood, a homogeneous medium that is connected to the central volume by flow. Venous equilibration is assumed, namely the venous drug concentration is in equilibrium with that in the organ.[2,3] Then organ-tissues are interconnected by the circulation and are put in place anatomically.[1]

Several important variables, including blood flow, plasma and red blood cell binding and transporter and enzyme activities have been identified as the determinants of organ clearance.[3-8] Simple PBPK models have been applied to describe data from the liver,[2,3,9] kidney,[10-12] intestine,[13,14] and whole body.[1,15,16] Several important variables, including blood flow, plasma and red blood cell binding, and transporter and enzyme activities have been identified as the determinants of organ clearance.[3-8] The PBPK model for the liver is based on the liver as the only eliminating organ in a situation akin to the recirculating perfused rat liver preparation (Figure 1A).[2] The model has been extended to

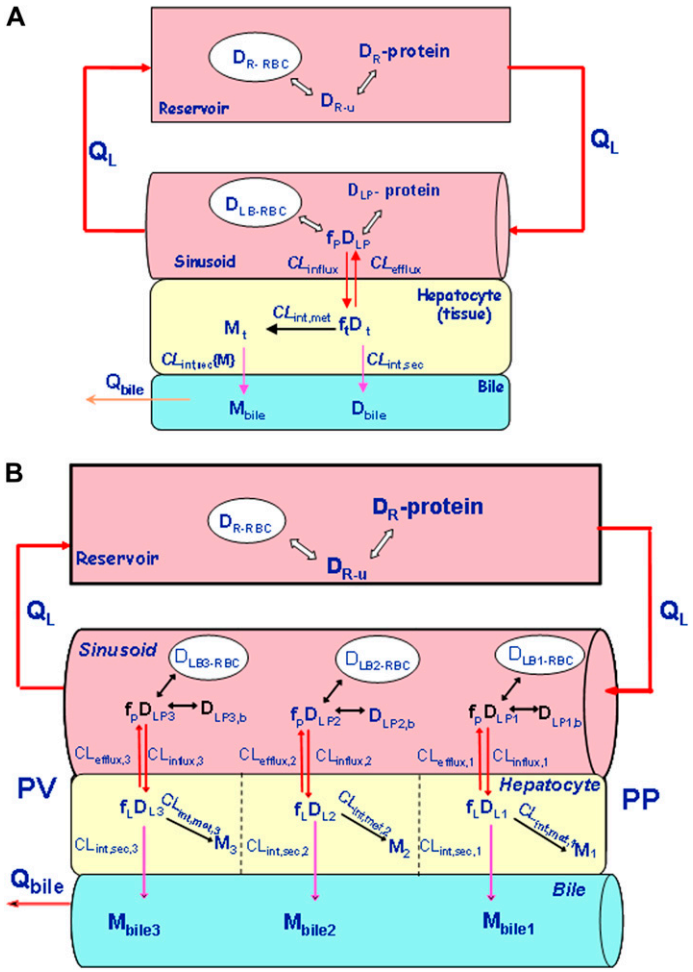

Figure 1. The simple physiologically based pharmacokinetic model (PBPK) (A) and zonal liver model (ZLM) (B). In the PBPK model (A), the liver compartment consists of the liver blood, tissue and bile compartments. Influx (CL_{influx}) and efflux (CL_{efflux}) clearances, as well as the metabolic ($CL_{int,met}$) and secretory ($CL_{int,sec}$) intrinsic clearances regulate levels of drug in tissue (D_L), plasma (D_P) and reservoir (D_R). M_{LB} is total amount of metabolite formed, including the amounts of metabolite in reservoir, bile, and liver tissue as well as those for subsequently formed metabolites; Q_L and Q_{bile} are the liver blood flow and bile flow rates, respectively. In the ZLM (B), the liver is divided into 3 zones (PP zone or zone 1, middle zone or zone 2, and PV zone or zone 3) according to the hepatic microcirculation. Subscript "i" denotes the influx ($CL_{influx,i}$), efflux ($CL_{efflux,i}$) and metabolic ($CL_{int,met,i}$) and secretory ($CL_{int,sec,i}$) intrinsic clearances in different zones. The sum of the all the activities in the zonal compartments provides the total intrinsic clearance for transport or metabolism. The models may further be modified to describe red blood cell (rbc) partitioning and binding to plasma proteins such as albumin (alb), expressed as the unbound fraction in plasma, f_p.

describe metabolism, excretion, and transport.[8] Processes describing carrier-mediated or passive transport are denoted by the influx and efflux clearances (CL_{influx} and CL_{efflux}) representing the activities of the basolateral transporters and passive diffusion. Sinusoidal transporters such as the sodium-dependent cotransporting polypeptide (NTCP), the organic anion transporting polypeptides (OATPs), and the organic anion (OAT2) and cation (OCT1) transporters facilitate influx (Figure 2).[5,7,9] Basolateral efflux at the lateral membrane occurs via MRP3 or MRP4, multidrug resistance-associated transporters 3 and 4 (Figure 2).[17-19] Biliary excretion is mediated via canalicular, ATP binding cassette (ABC) transporters such as the multidrug-resistance protein 1 (MDR1), also known as the P-glycoprotein (Pgp), the multidrug-resistance–associated protein 2 (MRP2), the bile salt export pump (BSEP), and breast cancer resistance protein (BCRP). In addition, drugs may be metabolized by phase I enzymes such as the cytochrome P-450s, and phase II enzymes such as the sulfotransferases (SULTs), UDP-glucuronosyltransferases (UGTs), and glutathione S-transferases (GSTs). The activities or the intrinsic clearances for biliary excretion by the ABC canalicular transporters and enzymes are denoted by the secretory ($CL_{int,sec}$) and metabolic intrinsic clearance ($CL_{int,met}$), respectively (Figure 2A).[2,5,7,8,20] Ordinarily, in vitro transport and metabolic studies provide estimates of the V_{max} (maximum velocity) and K_m (Michaelis-Menten constant) for uptake and metabolism. The ratio of V_{max}/K_m for uptake then furnishes estimates of the influx clearance (CL_{influx}), whereas that for V_{max}/K_m from metabolic studies provides the metabolic intrinsic clearance, $CL_{int,met}$.[2,21,22] It is often difficult to estimate the $CL_{int,sec}$ since the drug needs to have entered the cell and the (unbound) cellular concentration needs to be known to relate to the biliary excretion rate.

The advantage of modeling is that mathematical expressions that relate to flow, binding, and transporter and enzymatic activities are derived by matrix inversion for linear conditions. Solutions for clearances were found for the liver

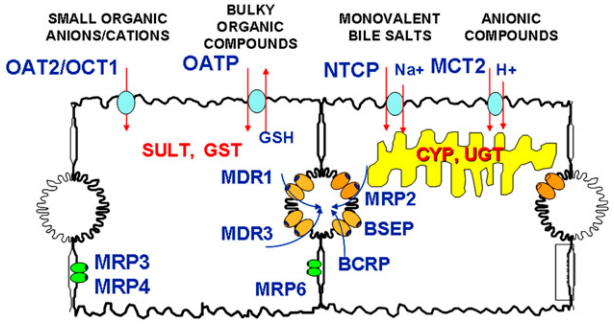

Figure 2. Schematic diagram of transport and metabolism of drugs in the hepatocyte that shows influx transporters, such as OATP, NTCP, OAT2, OCT1, and MCT2 at the sinusoidal membrane, and efflux transporters such as MRP3, MRP4, and MRP6 at the basolateral membrane, and efflux transporters, such as Pgp or MDR1, MDR3, MRP2, BSEP, BCRP at the canalicular membrane. The enzymes, such as CYP, UGT, SULT, and GST are present to mediate intracellular metabolism (reproduced with permission).[7] Set text for definition of terms.

PBPK model (Figure 1A). As shown below, the metabolic ($CL_{liver,met}$), biliary ($CL_{liver,ex}$), and total hepatic ($CL_{liver,tot}$) clearances relate to CL_{influx}, CL_{efflux}, $CL_{int,sec}$, $CL_{int,met}$, flow (Q_L), and the unbound fraction in blood (f_b).[20]

$$CL_{liver,met} = \frac{Q_L f_b CL_{influx} CL_{int,met}}{Q_L (CL_{efflux} + CL_{int,met} + CL_{int,sec}) + f_b CL_{influx} (CL_{int,met} + CL_{int,sec})} \quad (1)$$

$$CL_{liver,ex} = \frac{Q_L f_b CL_{influx} CL_{int,sec}}{Q_L (CL_{efflux} + CL_{int,met} + CL_{int,sec}) + f_b CL_{influx} (CL_{int,met} + CL_{int,sec})} \quad (2)$$

$$CL_{liver,tot} = \frac{Q_L f_b CL_{influx} (CL_{int,met} + CL_{int,sec})}{Q_L (CL_{efflux} + CL_{int,met} + CL_{int,sec}) + f_b CL_{influx} (CL_{int,met} + CL_{int,sec})} \quad (3)$$

It is readily seen that the total clearance ($CL_{liver,tot}$) is the sum of the metabolic ($CL_{liver,met}$) and biliary ($CL_{liver,ex}$) clearances. Upon division of Equation 1 by Equation 2, it may be deduced further that the ratio of the metabolic to biliary clearance is the ratio of $CL_{int,met}$ to $CL_{int,sec}$.[5,7]

$$\frac{CL_{liver,met}}{CL_{liver,ex}} = \frac{CL_{int,met}}{CL_{int,sec}} \quad (4)$$

From perfusion or in vivo studies, $CL_{int,sec}$ may be estimated indirectly from Equation 4 when the ratio of the metabolic/biliary clearance, as well as $CL_{int,met}$, is known. With knowledge of the binding parameter, f_b (unbound fraction in blood, estimated as the unbound plasma fraction, f_p, divided by the blood to plasma concentration ratio, [C_{blood}/C_{plasma}]), the only unknown left is the efflux clearance (CL_{efflux}). The parameter may be estimated from fitting.

Zonal Liver Model

It is notable, however, that hepatic enzymes and transporters are distributed in varying abundances among hepatocytes or zonal regions (Table 1).[23-39] The appropriate modification to accommodate this complexity is use of a zonal liver model (ZLM), the expanded counterpart of the PBPK model (Figure 1B).[7,34] Zones of the liver are denoted as subcompartments to include heterogeneity of transporters and enzymes. The ZLM describes zones 1, 2, and 3 that correlate to the periportal, midzonal, and perivenous zones of the acinus, the simplest microcirculatory unit (Figure 1B).[40] As may be envisioned, transporters are mostly distributed evenly; whereas many enzymes are not (Table 1). In the ZLM, the total activity for each sinusoidal influx or efflux transporter is simply the sum of those from individual zonal regions; the same may be said about the enzyme for metabolic activity and the canalicular transporter for excretory activities. For evenly distributed activities, the zonal activity for each acinar region is approximated by dividing the total transporter activity or intrinsic clearance for transport by 3. For uneven distributions, the zonal activity may

Table 1. Heterogeneous Distribution of Enzymes and Transporters in Rat Liver[7,23,24]

	Periportal	Perivenous	Reference
Cytochrome P-450 (Cyp)	Lower	Higher	23-25
UDP-Glucuronosyltransferase (Ugt)	Lower	Higher	26
Sulfotransferase			
Sulfotransferase 1a1 (Su1t1a1)	Even	Even	27
Hydroxysteroid sulfotransferase (Sult2a1)	Higher	Lower	28
Estrogen sulfotransferase (Sult1e1)	Lower	Higher	29
Glutathione S-Transferse (Gst)	Lower	Higher	30
Sulfatase	Even	Even	29,31
Sodium-dependent taurocholate cotransporting polypeptide (Ntcp)	Even	Even	32
Organic anion transporting polypeptide 1a1 (Oatp1a1)	Even	Even	33
Organic anion transporting polypeptide 1a4 (Oatp1a4)	Even	Even	34
	Lower	Higher	35
Organic anion transporting polypeptide 1b3 (Oatp1b3)	Lower	Higher	36
Organic cation transporter 1 (Oct1)	Lower	Higher	37
Bile salt export pump (Bsep)	Even	Even	38
Multidrug resistance protein 1 (Mdr1) or P-glycoprotein (Pgp)	Even	Even	34
Multidrug resistance-associated protein 2 (Mrp2)	Even	Even	30
Multidrug resistance-associated protein 3 (Mrp3)	Lower	Higher	39

be presented as a percentage of the total intrinsic clearance or activity.

Many success stories may be told with the PBPK model and the ZLM, as exemplified by the data on enalapril,[8,41] salicylamide,[42,43] morphine,[44] estrone sulfate,[45] estradiol 17β-D-glucuronide ($E_2$17G),[9] and digoxin[34] from rat liver perfusion studies. It cannot be overemphasized that much of the success relies on defining the red blood cell and protein-binding data from in vitro experiments, then examination of transporter/metabolic (S9/microsome/cytosol) activities with isolated (homogeneous and zonal) hepatocytes, and transporter/enzyme protein levels with immunoblotting.

Digoxin

Digoxin (Dg3), which displays red cell carriage and modest protein binding, is taken up by the Oatp1a4, excreted by Mdr1 (or Pgp), and metabolized by Cyp3a2 to the bis- and mono-digitosoxides and digitoxigenin in the rat liver.[34] The immunoblots on protein levels of Oatp1a4 for uptake and Pgp for excretion suggest lack of zonal transport of digoxin among rat periportal and perivenous rat hepatocytes.[34] With these background information on hand, the fit of the digoxin data arising from rat liver perfusion experiments, performed in the absence and presence of albumin and red cells in perfusate, to the PBPK model showed excellent results (Figure 3).[34] From modeling, the rate-determining step in controlling digoxin clearance was discerned to be protein binding and not enzyme or transporter activity. Additional information on the expression of protein levels of enzymes and transporters and their acinar distributions served as vital data for the ZLM. With the known perivenous distribution of Cyp3a2 (expressed as a percentage of total $CL_{int,met}$) and the even distribution of transporters (Oatp1a4 and Pgp) for the ZLM, the fit only improved nominally, showing that heterogeneity is not an important factor, since digoxin is a poorly cleared by the rat liver.

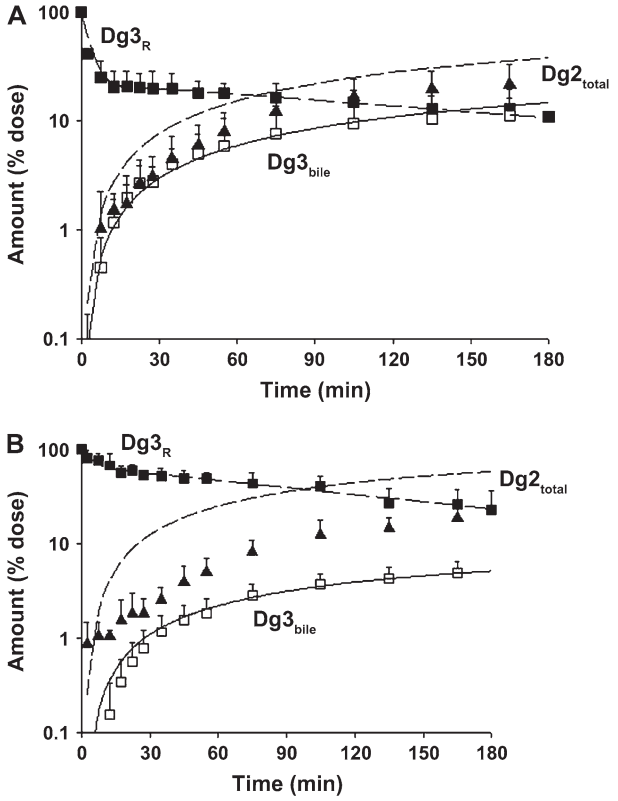

Figure 3. Fits of the Dg3 (digoxin) data in reservoir ($Dg3B_{RB}$) (■) and bile ($Dg3B_{bileB}$) (□) to the PBPK model for the (A) KHB-perfused (without rbc or albumin for binding) and and (B) rbc-alb-perfused (with binding) livers. Dg2 (▲) represented summed amounts of all of the metabolites in reservoir and bile (% dose), but not those in liver (> 40% dose). Therefore, the total amount of metabolite (Dg2) was predicted rather than fitted, and the predicted amount of metabolite formed ($Dg2_{total}$) was underestimated since Dg2 amounts in liver was not accessible. Reproduced with permission.[34]

Estradiol 17β D-glucuronide ($E_2$17G)

The contrasting example is $E_2$17G, a model substrate that is highly cleared in the rat liver because of rapid sinusoidal and canalicular transport by the Oatp1a1, Oatp1a4, and Oatp1b2, and Mrp2, respectively, and sulfation by estrogen sulfotransferase (Sult1e1).[9] The 3-sulfated metabolite, $E_2$3S17G, fails to traverse the basolateral membrane for both influx and efflux, but undergoes desulfation and therefore futile cycling with $E_2$17G. Avid excretion of $E_2$3S17G and $E_2$17G occurs with Mrp2. In Wag/Rij rats that developed liver metastasis upon intraportal injection of CC531 colon adenocarcinoma cells, sinusoidal transporters, Oatp1a1 and Oatp1b2, were reduced (40% loss), whereas Sult1e1 was induced (40%) compared with those in the sham-operated livers.[9] These occurrences were well described by the PBPK model fit of data obtained in liver perfusion studies (Figure 4).[9] The reduction in sinusoidal activity proved to be irrelevant since basolateral entry of $E_2$17G was so rapid (> 40× blood flow rate) that, despite a reduction of transport with tumor, uptake of $E_2$17G was maintained rapid enough (> 20× blood flow rate). In contrast, induction of Sult1e1 in tumor livers increased $E_2$3S17G formation, and evoked compensatory decreases in the biliary excretion of $E_2$17G, although the activities of Mrp2 that excretes both $E_2$17G and $E_2$3S17G were unchanged (Figure 4A).[9] These observations highlight the interplay between the enzyme and canalicular transporter; increased metabolism evoked a compensatory decrease in excretion even though Mrp2 activity remained unchanged. The zonal Sult1e1 activities toward estrone sulfation were known[29]; the ratio of Sult1e1 activities in periportal versus perivenous hepatocytes was 1:4. Taking the assumption that the same existed for $E_2$17G sulfation, enzymic heterogeneity of Sult1e1 was predicted as an important

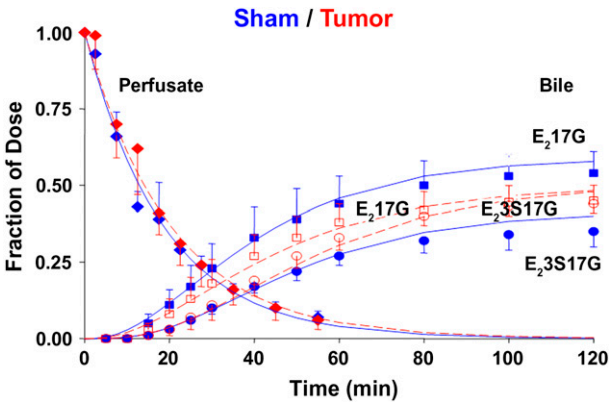

Figure 4. Fits of liver perfusion data: $E_2$17G in reservoir perfusate from metastatic tumor-bearing (n = 5, ◆) and sham-operated (n = 4, ◆) livers at 4-week postdevelopment of inoculation of CC531 cells and PBS, respectively, to a PBPK model. Higher amounts of $E_2$17G (■) were excreted unchanged in sham livers versus tumor livers (□). The metabolite, $E_2$3S17G, appeared only in bile, reflecting the amounts (fraction of dose) formed from sham (●) and tumor (○) livers. Perfusate $E_2$17G (◆,◆) levels were unchanged even though sinusoidal influx by Oatp1a1 was decreased. By contrast, the cumulative amounts of $E_2$3S17G (○ vs ●) were higher, and $E_2$17G (□ vs ■), lower, in tumor livers due to the increased Sult1e1 with tumor. Fits to the data with the PBPK model (blue and red lines) adequately predicted both sets of data with increased Sult1e1 (40%) but decreased Oatp1a1 (40%). Reproduced with permission.[9]

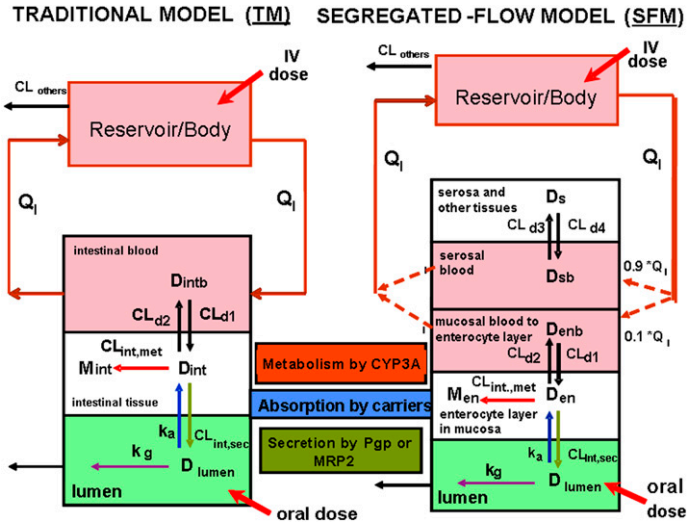

Figure 5. Fates of drug (D) and metabolite (M) in the TM (A) and SFM (B). Note that the entire oral dose passes through the enterocyte region for both the TM and SFM, whereas only a partial intravenous dose reaches the enterocyte region for the SFM. For TM, the intestinal blood (Q_l) perfuses the entire intestinal tissue, the site of metabolism and absorption from the lumen. For SFM, intestinal blood is segregated to perfuse the non-metabolizing and enterocyte-mucosal regions. Drug equilibrates with those in the corresponding tissue layers with intrinsic transfer clearances CL_{d1} and CL_{d2} for TM, or CL_{d1} and CL_{d2}, CL_{d3} and CL_{d4} for SFM. The absorptive, metabolic and efflux activities within the villus tips of the mucosal layer are represented by the rate constant, k_a, and metabolic and secretory intrinsic clearances, $CL_{int,met}$ and $CL_{int,sec}$, respectively. Gastrointestinal transit is denoted by CL_{GIT}. Adapted from reference 14, with permission.

factor in $E_2$17G elimination. This is because $E_2$17G is highly cleared by the rat liver.[7]

Intestinal Models

Physiologically based models have been used to describe data for intestinal absorption, secretion, and metabolism. The simple, physiologically based or traditional model (TM) was first used to explain the metabolism of morphine to morphine 6-glucuronide in the perfused small intestine preparation (Figure 5). The TM was then modified to the segregated flow model (SFM) (Figure 5) in order to explain the preferential metabolism of morphine, given orally versus systemically[13]; the phenomenon is known as route-dependent intestine metabolism.[46] The SFM entails a split flow to the enterocyte region and the remainder of the intestine, and suggests that a low proportion of the intestinal blood supply (5% to 30%, assigned as 10% for sake of simplicity) enters the enterocyte or active region for absorption, efflux, and metabolism. The SFM is superior to the TM in explaining the absence and presence of morphine glucuronidation when given systemically and orally, respectively, to the perfused rat intestine preparation (Figure 6).[13,46]

As in the liver, intestinal enzymes and transporters are involved (Figure 7), and these are also heterogeneously distributed among segments (Table 2).[47-62] Segmental and segregated flow models (STM for segmental, tradition model, and SSFM for segmental, segregated flow model) have been applied to incorporate heterogeneity in flow, enzymes, and transporters along the small intestine (Figure 8).[63] Basically, the TM and SFM are expanded to 3 segmental regions receiving parallel artery blood supply. The SSFM aptly explains route-dependent intestinal elimination and incorporates segmental distribution of enzymes and transporters in drug absorption. Heterogeneity was noted for Cyp3a and Pgp, a major contributor for digoxin efflux, among the segments (Figure 8), although both Pgp and Cyp3a (mostly Cyp3a9 and Cyp3a62 in intestine,[64] detected by the antibody) were induced by pregnenolone 16α-carbonitrile (PCN), a ligand of PXR, the pregnane X receptor. Digoxin removal was found to be mediated only via Pgp in the perfused rat intestine since levels of Cyp3a2 are low in the intestine.[64] The total activity (aggregate of the relative intensities of all the segments) may be found by summation of protein/segment × intensity/μg protein; then the relative intensity for duodenal, jejunal, or ileal segment, divided by the total relative intensity of the intestine, would provide the

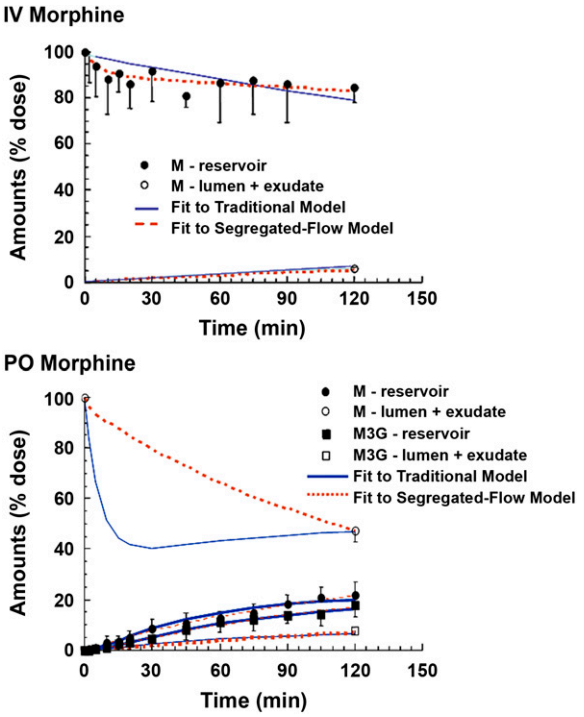

Figure 6. Fits of tracer [^{3}H]morphine data (●) from the vascularly perfused recirculating, rat small intestine preparation to the TM and SFM, after systemic dosing into the reservoir (upper panel) and oral administration into the duodenal lumen (lower panel).[14] There was a total lack of morphine glucuronide formed with intravenous dosing; only morphine (○) was detected into the lumen (and luminal fluid that was collected as exudates). By contrast, morphine glucuronide was detected in perfusate (■) and luminal fluid (□) with oral dosing (lower panel). Note the superior fit of the data to the SFM (– – – –) over the TM (————). Adapted from reference 14, with permission.

fraction of the total activity, and yields the fractional intrinsic clearance for metabolism or excretion. Upon modeling first with the SFM with an unstirred water layer exiting in the lumen, the intravenous and oral data of digoxin were predicted well by the SFM (Figure 9). When the heterogeneity of Pgp was factored in for purposes of simulation, the prediction was only slightly improved, since digoxin is poorly cleared by Pgp and metabolism was virtually absent in the rat intestine. In this case, the SFM or even TM suffices and the SSFM need not be evoked.[34] These examples are successful accounts that data on transporters and enzymes, with and without induction, may be explained by data in the perfusion system, and are adequately described by physiologically based and segmental models.

Circulatory Models

Although circulatory models were introduced into pharmacokinetics more than 25 years ago,[65,66] less than ~1% of the

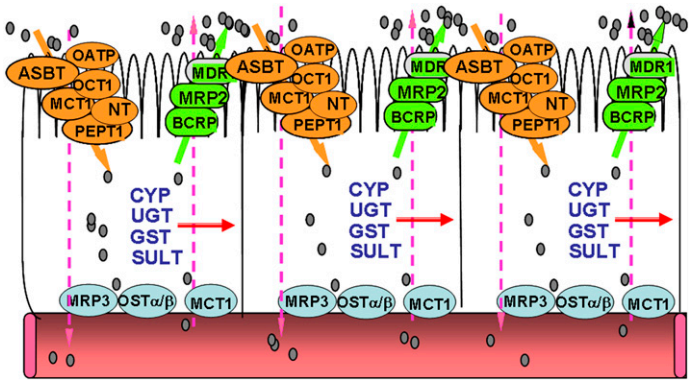

Figure 7. Transporters (apical absorption and efflux, and basolateral efflux) and enzymes in the intestinal segments, the duodenum, jejunum, and ileum. Heterogeneity also exists in their segmental distribution.

models used since then analyze clinical pharmacokinetic data that obey a circulatory structure. The relevance of circulatory models in whole-body pharmacokinetics appears justified since the underlying transport processes are primarily advective transport to the organs or tissues and diffusion within organs, and one could argue that the fundamental role of circulatory drug transport should imply a recirculatory model. However, the decisive question is not the truth of the models but their adequacy for solving a certain task, or according to an often-quoted statement by George Box: "all models are wrong but some are useful" (*Robustness is the Strategy of Scientific Model Building*, 1979) ("wrong" in the sense that all models are simplifications of reality). Thus, the practical question is: why and when are circulatory models more useful than traditional models? The rationale behind the use of mammillary compartmental models in pharmacokinetics is the modeling of drug distribution in the body. A drawback of conventional models is that these compartments lack physiologic reality, and distribution parameters cannot be readily interpreted in terms of underlying transport mechanisms, ie, advective transport by blood flow (vascular mixing), transcapillary transport (permeation), and tissue-binding kinetics. Thus, these models fail to describe the time course of drug concentration within the first 2 minutes following bolus injection (including the role of the lung) because of the assumption of instantaneous mixing in the central compartment. In contrast, recirculatory models with compartmental subsystems adequately characterize the initial mixing phase and the pulmonary first-pass effect, and are of special importance for fast-acting drugs like intravenous anesthetics. In addition to intravascular mixing, a minimal circulatory model in which all organs of the systemic circulation are lumped into one heterogeneous subsystem may also account for transcapillary transport and intratissue diffusion of drugs, and are particularly useful to evaluate the distribution kinetics of drugs under the influence of disease states.

Table 2. Heterogeneous Distribution of Enzymes and Transporters in the Small Intestine

	Duodenum	Jejunum	Ileum	Reference
Cytochrome P-450 (rat, humans)	Higher		Lowest	47-49
UDP-Glucuronosyltransferase (rat)	Higher		Lowest	50
Sulfotransferase (guinea pig)	Higher		Lowest	51
Glutathione S-transferase (rat)	Highest		Lowest	52
Sulfatase (rat)	Highest		Lowest	53
Oligopeptide transporter 1 - PEPT1 (rabbit)	Highest			54
Apical sodium-dependent bile acid transport - ASBT (hamster, rat)	Lowest		Highest	55,56
Monocarboxylic acid transporter 1 - MCT1 (rat)	Lower	Highest	Lowest	57
Organic anion transporting polypeptide 3 - Oatp3 (rat)	Lower	Higher	Lower	58
Multidrug resistance protein MDR1 or Pgp (rat)	Lowest	Higher	Highest	59
Multidrug resistance-associated protein 2 - MRP2 (rat)	High	Highest	Lowest	60
Multidrug resistance-associated protein 3 - MRP3 (rat)	Lowest	Higher	Lighest	61,62

A condition that limits the complexity of models of solute distribution in the body is that they must be theoretically and practically identifiable while remaining consistent with known physiology. An implicit assumption in the use of the term "circulatory" pharmacokinetic models is that the parameters can be estimated on the basis of plasma concentration–time data, and are readily applicable to clinical data. The so-called PBPK models, in contrast, also have a circulatory structure but are typically too complex for identification on the basis of plasma concentration time data alone.[67]

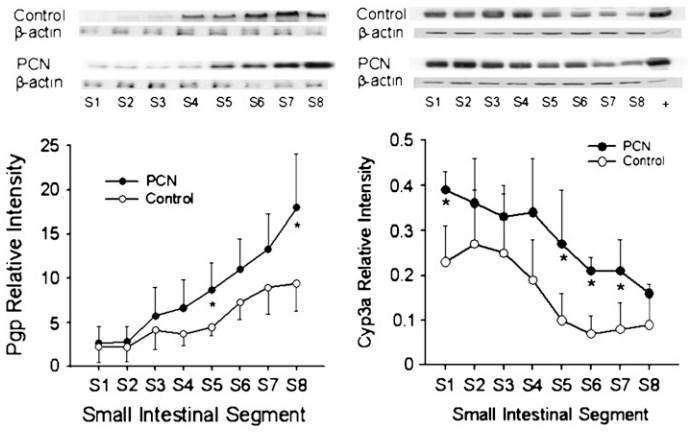

Figure 8. Heterogeneity of Pgp (left panel) and Cyp3a (right panel), detected in enterocyte membrane fragments along segmental regions of the rat small intestine by Western blotting. S1 denotes the duodenum, S2, the proximal jejunum of equal length as S1; S8 is the distal ileum, and S3-S8 are segments of equal lengths, with S2 – S7 representing the jejunum. Both Pgp and Cyp3a were induced by PCN (pregnenolone 16α-carbonitrile), a ligand of the pregnane X receptor, PXR. The symbol "*" denotes $P < .05$. Taken from reference 59, with permission.

Initial Distribution

Circulatory models have been successfully used to evaluate the distribution kinetics of fast-acting drugs, and to relate them to the onset and offset of action. Thus, it is now well recognized that modeling of drug distribution kinetics within the first 2 minutes (front-end kinetics) determines the induction dose of intravenous anesthetics.[68,69] A recirculatory model with a chain of compartmental subsystems that adequately characterizes pulmonary first-pass distribution and intravascular mixing has been applied to analyze the kinetics of inulin, antipyrine, lidocaine, and thiopental.[70-72] This model uses plasma concentration time data, in the absence of destructive sampling, to describe the effect of changes in hemodynamics attributable to drug interaction[71] or hemorrhagic shock[73] on whole body pharmacokinetics. In a PK/PD analysis of rocuronium, Kuipers et al[74] showed that circulatory models accounted for the effect of cardiac output and allowed an improved estimation of pharmacodynamic parameters. Similar circulatory models with compartmental subsystems have been applied to propofol[69,75] and fentanyl.[76] A prerequisite of such studies is a high frequency of arterial blood sampling during the first minutes after rapid drug injection and the concomitant administration of a vascular marker, indocyanine green (ICG). From the ICG disposition data, cardiac output and blood volume can be estimated. Although the latter is the initial mixing volume of the drug, this process does not occur instantaneously, with the consequence that the initial distribution volume (well-mixed plasma compartment) as defined in mammillary compartmental models is fictitious. It is often overlooked that for highly extracted drugs this simplification may lead to errors in clearance estimation.[77] It should be noted that instantaneous initial mixing is also an implicit assumption of the use of monotonically decreasing disposition

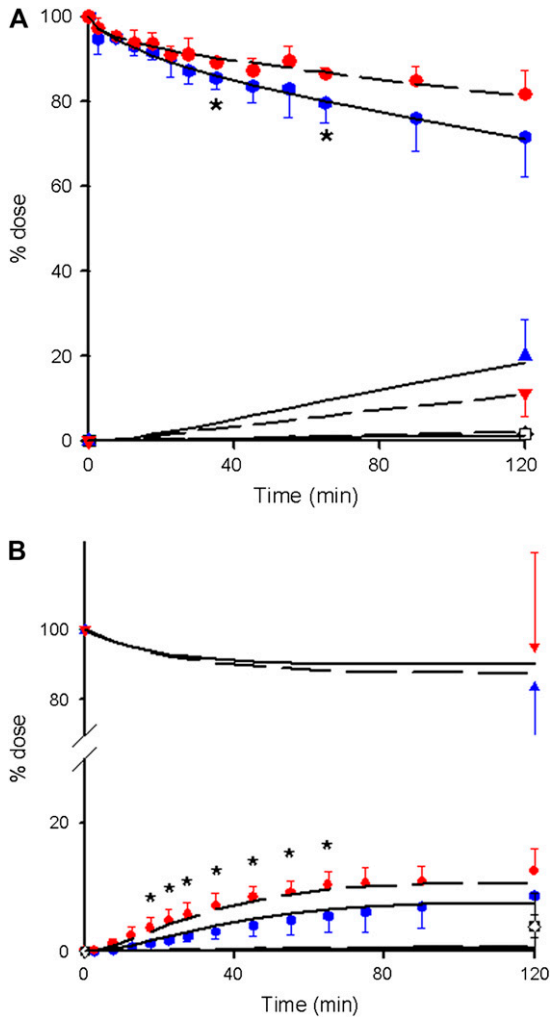

Figure 9. Fit of the intestinal perfusion data of digoxin (Dg3) for intravenous (A) and oral (B) dosing, with (●, blue symbols) and without (●, red symbols) PCN treatment, to the SFM; an unstirred water layer needed to be added to the SFM model.[59] Avid secretion of digoxin (▲,▼) but little digoxin metabolism to DG2 (□) was observed. Predictions from the SFM matched the observations on PCN-treated (——) and control (– – –) experimental data well. The symbol "*" denotes $P < .05$. Taken from reference 59, with permission.

curves (eg, multiexponential functions). If drug input is slower than the initial distribution process (short-term infusion), the effect of the latter is reduced or lost. Thus, simpler recirculatory models and less frequent sampling are sufficient in this case,[78,79] especially when an independent estimate of cardiac output is available.

Circulatory Models with Heterogeneous Subsystems

Because circulatory models with compartmental subsystems can be described by a set of ordinary differential equations simplifies mathematical modeling, since most available software for parameter estimation allows model representation by differential equations. This does not hold, however, for nonhomogeneous subsystems, ie, the modeling of dispersion and diffusion processes. A mathematical tool that is independent of the underlying specific structural model can be found in the theory of residence or transit time distributions. The equation for the arterial concentration–time curve after rapid bolus injection (dose D_{iv}) of the drug is available in the Laplace domain as a function of transit time densities (TTD) across subsystems, the pulmonary circulation, $\hat{f}_p(s)$, and the systemic circulation, $\hat{f}_s(s)$[78]:

$$\hat{C}(s) = \frac{D_{iv}}{Q_{body}} \frac{\hat{f}_p(s)}{1-(1-E_{sys})\hat{f}_s(s)\hat{f}_p(s)} \qquad (5)$$

where Q_{body} is cardiac output and E_{sys} the extraction ratio of drug in the systemic circulation (Figure 10). A method of numerical inverse Laplace transformation must be implemented in a nonlinear regression software for parameter estimation and model simulation. Independent of its use in data analysis, a stochastic circulatory model can serve as a basis for developing a mechanistic approach to drug distribution in the body.[80] It can be shown that vascular mixing is a result of mechanical dispersion in the microcirculatory network. An appropriate TTD of the vascular marker is the inverse Gaussian density,[81,82] known as the first passage time of a random walk process with drift. Since the latter evolves as a solution to the convection-dispersion equation,[83] it is not surprising that circulatory mixing models can also be based on this equation.[84,85] The circulatory minimal model (Figure 10 and Equation 5) has been successfully applied to the data of ICG and unbound drugs,[82] including sorbitol (Figure 11). Processes that govern tissue distribution kinetics of drugs, such as capillary permeation and intratissue diffusion (and/or binding), further increase the relative dispersion of transit times.[82,86] While the mean

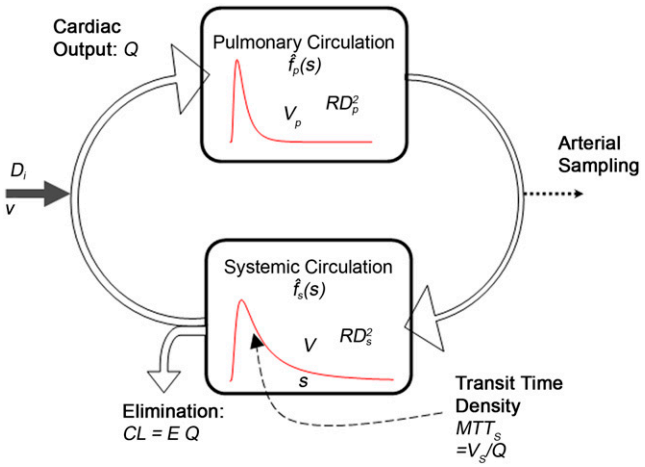

Figure 10. The circulatory, minimal model with inverse Gaussian density used to analyze disposition kinetics of ICG, inulin, antipyrine, and sorbitol.

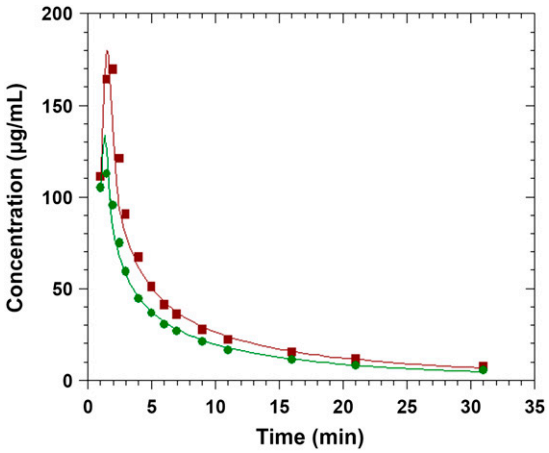

Figure 11. Fits of the circulatory model (Fig. 10 and Equation 5) to sorbitol plasma concentration–time data as observed for a 1-minute infusion 0.8 g sorbitol in a human volunteer under control conditions (■) and after infusion of orciprenaline (●) leading to a 50% increase in cardiac output (Weiss M, Huebner G, Sziegoleit W, unpublished data, 2000).

transit time and flow determine the distribution volume, the relative dispersion of TTD and flow determine distribution clearance.[78,82,87] The model describes the change from flow- to diffusion-limited distribution as a continuous transition.[87] Thus, apart from its ability to describe initial mixing, a circulatory model provides a framework that allows for quantitative assessment of processes governing distributional equilibrium in the body. It can be used to define the total distribution clearance of a drug as a parameter of distribution kinetics, which has a clear physical meaning.[78,82]

Nonhomogeneous Sampling Compartment

Since circulatory models can account for concentration differences within the vascular space, they are useful for the analysis of plasma concentration–time data obtained at different sampling points, eg, when portal and systemic blood samples were simultaneously taken to evaluate intestinal absorption[88] and/or to characterize the role of the liver.[89] The transient concentration difference between arterial and peripheral venous blood concentration, on the other hand, have to be taken into account in PK/PD modeling.

Fractal Pharmacokinetics

Kinetic processes are traditionally interpreted with classical kinetics that is quite satisfactory for reactions and processes in well-stirred media. The kinetics of diffusion-controlled processes and reactions in 3-dimensional homogeneous systems obey the classical laws of diffusion where the rate constant of the process is linearly proportional to the diffusion coefficient. However, this proportionality is no longer valid for systems with smaller dimensions, namely, fractal spaces or disordered systems, since the laws of transport are different in these media. Accordingly, fractal kinetics has been developed since classical kinetics has been found to be unsatisfactory under dimensional constraints, eg, phase boundaries, understirred media, or membrane reactions.

Classical models used in biopharmaceutics, pharmacokinetics, and pharmacodynamics rely on the concept of *homogeneity*. For example, the compartments in multicompartmental PK/PD models are considered homogeneous and well mixed. However, the most compelling feature of physiological systems is their complexity. The assumptions of homogeneity and well-stirred media are contrary to the evidence provided by the anatomical and physiological complexity of the human body. Thus, many diffusion-controlled drug processes take place in understirred media, where the rate constant of the process is not linearly proportional to the diffusion coefficient. A diffusion process under such conditions may be highly variable since the laws of transport are different in these media. A general well-known result is that in constrained spaces, diffusion is slowed down and follows an anomalous pattern. A better description of transport limitations can be based on the principles of diffusion in disordered media.[90] Thus, concepts from fractal geometry[90] and fractal kinetics[91,92] can be used to achieve a more realistic modeling of the complex and the kinetically heterogeneous phenomena.[93] Table 3 provides a list of the basic classical and nonclassical considerations accompanying the study of the in vitro and in vivo processes. A review article focusing on the homogeneous and heterogeneous approaches used for the description of the various phenomena involved in the time-course of drug through the body has been published recently.[94] A brief description of the concepts of fractals and fractal kinetics are given here along with various applications in the fields of biopharmaceutics and pharmacokinetics.

Fractal Models for Drug Release, Dissolution, and Uptake

The assumptions of homogeneity and/or well-stirred media in the gastrointestinal (GI) tract are contrary to the evidence given the anatomical and physiological complexity of the

Table 3. Classical and Nonclassical Considerations of the In Vitro and In Vivo Drug Processes

Fields	Classical	Nonclassical
Geometry	Euclidean	Fractal
Topology	Ordered media	Disordered media
Diffusion	Regular	Anomalous
Kinetics	Deterministic	Stochastic
Dynamics	Linear	Nonlinear

GI tract. All processes related to GI drug absorption, ie, drug release, dissolution, transit, and uptake are heterogeneous since they take place at interfaces of different phases (solid-liquid or liquid-membrane) under topological constraints (variable and understirred conditions). As the drug moves down the intestine, the flow is forced in the narrow and understirred spaces of the colloidal contents and therefore friction becomes more important than intermolecular diffusion. The characteristics of this type of flow have been studied with Hele-Shaw channels ensuring a quasi 2-dimensional space using miscible fluids of different viscosities.[95,96] These studies revealed that viscous, fractal fingers are formed under these topological constraints, which have also been observed in experiments dealing with the secretion of HCl and its transport through the mucus layer over the surface epithelium under in vitro and in vivo conditions.[97,98] In light of these observations, drug absorption phenomena have been interpreted in terms of fractal concepts.[99] It was proposed that the transit, dissolution, and uptake of drug under the heterogeneous GI conditions obey the principles of fractal kinetics.[92] For this type of kinetics, the rate "constants" depend on time:

$$k = k_0 t^{-\lambda} \tag{6}$$

where k is the rate coefficient, k_0 is a constant, and the exponent, λ, is different from zero and is the outcome of 2 different phenomena: the heterogeneity (geometric disorder of the medium) and the imperfect mixing (diffusion-limit) condition. In this vein, the "absorption rate coefficient," which is compatible with the time-dependent character of the process, was proposed to replace the classic notion of "absorption rate constant."[99] Reports of 2 studies showed that time-dependent absorption models were used to interpret the GI absorption of cyclosporine A[100] and propanolol.[101] Moreover, Monte Carlo techniques that incorporate the heterogeneous features of the GI wall structure and of the drug flow have been used to characterize the intestinal drug transit, dissolution, and uptake.[102,103] It is also worthy to mention recent findings on the chaotic nature of the gastric myoelectrical complex.[104] Thus, the frequently observed high variability in gastric emptying data should not be attributed exclusively to the classical randomness of rhythmic electrical oscillation in the stomach. Plausibly, one can argue that this will have an immediate impact on the absorption of highly soluble and highly permeable drugs from immediate release formulations since their absorption is controlled by the gastric emptying rate.

In the fields of drug release and dissolution, several studies support the heterogeneous features of these processes. The empirical, wide, and successful application of the Weibull function[105] (Equation 7) in dissolution studies have been justified theoretically on the basis of fractal kinetics considerations.[106] Lansky and Weiss[107-109] introduced the concept of the nonconstant fractional dissolution rate and provided an index to quantify heterogeneity for various dissolution models. Also, a population growth model of dissolution based on a difference equation was developed.[110] The derivation of the recurrence equation of this model does not rely on Fick's first law of diffusion and the time continuity assumption and it has been used to explain classical and nonclassical (supersaturated) dissolution data.[110,111] Diffusion-controlled drug release has also been studied in Euclidean and fractal geometries using Monte Carlo techniques.[112-119] It was found[113,114] that the Weibull model (which is the exponential of a power law [ie, a stretched exponential function]) is:

$$\frac{M_t}{M_\infty} = 1 - \exp(-\alpha t^b) \tag{7}$$

where M_t and M_∞ are the amounts of drug released at times t and infinity, respectively, and α and b are constants. The equation describes quite well experimental and computer-generated data using Monte Carlo techniques; also, a physical meaning for α and b in Equation 7 was provided recently.[120] The exponent of time b originates from the fact that a depletion zone is created gradually near the boundaries of the release device, and thus, the concentration in the device is not uniform.

Pharmacokinetics, Drug Metabolism, and Disposition

In contrast to classical pharmacokinetics in which a compartmental system is made up of a finite number of compartments, each being homogeneous and well mixed and interacting by exchanging material, the essential materials and drugs in the human body are transported through space-filling fractal networks of branching tubes while the internal surface areas of organisms for material exchange are "maximally fractal."[121,122] These observations prompted Karalis et al[123] to conceive the body as a fractal object with an infinitely high surface-to-volume ratio in order to interpret the nonphysiological values (>70 L) of the apparent volumes of distribution of drugs. The effective exchange area in the internal structure of the body was linked to the so-called "fractal volume of drug distribution,"[123] which was recently associated with the body surface area used in dosage regimen design.[124] The clearance analog, called "fractal clearance," was also defined[125]; both novel parameters were used in quantitative structure pharmacokinetic relationships.[125-127] Additionally, the use of the scaling laws describing the fractal-like architecture of the arterial and venular trees enabled the development of a physiologically based model of 1-dimensional tube for the transport of materials in the circulatory system.[128] Figure 12 shows the geometrical transformation of the dichotomous branching network to an equivalent 1-dimensional tube, which corresponds to the

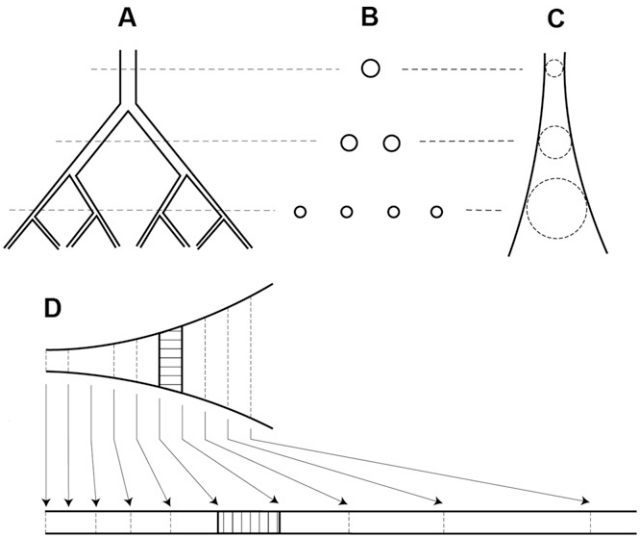

Figure 12. Transformation of the branching vascular tree to an equivalent 1-dimensional tube model. (A) Schematic representation of a dichotomous branching network. (B) Cross sections at each level. (C) Tree is replaced by a single tube with continuously increasing radius. The area of the cross section of the tube is equal to the total areas of the cross sections of each level of the tree. (D) Volume-preserving transformation of the varying radius tube (C) to a fixed radius tube. Reprinted from Dokoumetzidis and Macheras[128] with permission of Springer.

arterial, venular, and pulmonary trees successively. A dispersion-convection partial differential equation with constant coefficients was used to describe the heterogeneous concentration profile of an intravascular tracer (indocyanine green) in the vascular tree. This model was further applied to the estimation of recirculatory parameters.[85]

The deterministic definition of a compartment refers to a kinetically homogeneous amount of material. The equivalent stochastic definition is that the probability of a unit participating in a particular transfer out of a compartment, at any time, is the same in all units in the compartment.[93] This allows us to formulate stochastic compartmental models based on probabilities of transfer that can capture heterogeneity in pharmacokinetics. A model of this type has been developed for cyclosporine.[129] In parallel, the simplified notion of the classical homogeneous compartments used in pharmacokinetics has been questioned in the literature[130-134] and attempts have been made for a more realistic description of the heterogeneous features of drug distribution in the body. Two approaches, based on fractal kinetics principles, have been used to describe the pharmacokinetics of Ca^{2+} and amiodarone in deep tissues.[134,135]

The kinetics of drug metabolism in the human body is classically analyzed with the Michaelis-Menten (MM) formalism. Normally, the derivation and application of the MM equation presuppose that the substrate (drug)-enzyme reaction takes place in a well-stirred medium. However, many enzymes are now known to be localized within 2-dimensional membranes or quasi 1-dimensional channels. Thus, several approaches have been proposed for the analysis of the enzyme-catalyzed reactions under topological constraints.[136-138] Also, Monte Carlo simulations were used for the study of the enzymatic reaction in 2-dimensional lattices.[139] It was found that the micro-constant associated with the formation of the substrate-enzyme complex is a time-dependent reaction coefficient, ie, it crosses over from a constant region at short times to a power law decrease at longer times.[139] Fuite et al[140] were the first to incorporate a "fractal compartment" in a physiologically based pharmacokinetic model in order to explain the unusual nonlinear pharmacokinetics of mibefradil (Figure 13). This "fractal compartment" was associated with the fractal structure of the liver, which dictates the unusual kinetics of mibefradil. Monte Carlo simulations of the enzymatic reaction in a 2-dimensional lattice were also performed under conditions that mimic the in vivo recirculation of the reactant species, ie, drug and metabolite.[141] A modified version of the MM equation was derived from the Monte Carlo simulations and used to explain mibefradil pharmacokinetics. Recently, fractal MM kinetics under steady-state conditions was also applied to mibefradil pharmacokinetics.[142] Chelminiak et al[143] applied the theory of networks to investigate the effects of diseased states of the liver on its ability to clear a drug from the plasma. By varying the number of links and traps of the random network, different disease states of the liver related to vascular damage were simulated. This study is the first to describe the liver as a network of catalytic enzymes and attempts to quantify the ability of the liver to metabolize drug molecules under a range of conditions that reflect both normal and pathological conditions.[143]

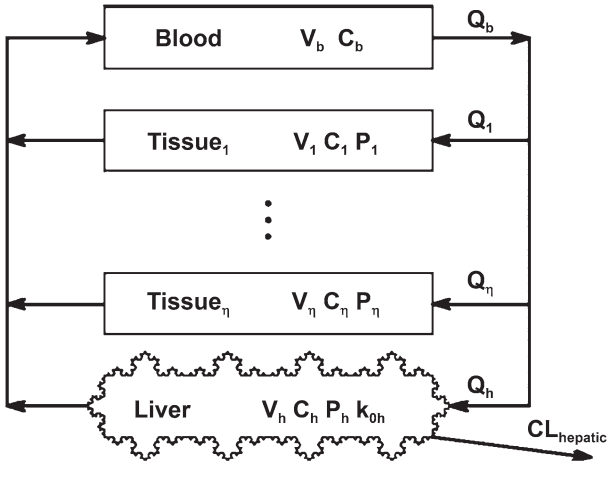

Figure 13. A physiologically based model developed by Fuite at al[140] in which a fractal compartment is used to represent the liver. Reprinted from Fruite et al[140] with permission of the American Physical Society.

Comparison of Models

We have described 3 advanced models that may use different forms of data and display different types of information. PBPK models are highly correlated with physiologically relevant structures and anatomical placements of organs in the body. The PBPK and ZLM for the liver and the SFM and SSFM for the intestine are structurally based models that further relate to zones of the liver and segments of the intestine in housing transporters and enzymes. These models use data on transporters and enzymes to reflect knowledge pathways controlling the time- and space-events in the organ and provide data that are more mechanistically based. The models relate to processes mediated by transporters, enzymes, flow, red cell, and protein binding, provide mechanistic information on the rate-limiting step, appraise changes in transporters or enzyme, and explain the interplay of transporters and enzymes. The physiological variables: weights, lengths, physiologic volumes, and attendant blood flow to each subcompartment (zone/segment) all need to be considered. Heterogeneity in transporters and enzymes among different compartments and homogeneous flow are adequately addressed. Changes in transporters and enzymes, as noted via protein characterization, are used for prediction in the physiologically based models, thereby providing mechanistic insight to biological events occurring within eliminating organs.

The PBPK model emphasizes an instantaneous equilibrium between spaces for distribution, transfer, and elimination. However, equilibration within each subcompartment and the blood compartment is deemed as instantaneous. This is not achieved in reality. In circulatory models, this assumption does not need to be made. The circulatory and fractal models relate more to stochastic events and incorporate heterogeneity in flow and organ structure. The model is able to account for the lack of immediate equilibration in blood, even at different locales and other tissue compartments. Circulatory models are more relevant if the goal of the study is to examine problems of drug distributional kinetics, eg, effects of changes in cardiac output, capillary permeability, tissue binding, and of concentration gradients within the circulation. Since the validity of a model is solely determined by the modeling objectives, traditional models should be sufficient in all other cases. The circulatory model has been developed for situations in which only blood/plasma concentration–time data are available in absence of tissue sampling, as in the clinical situation. Thus, the more important application of the model is in the definition of drug distribution kinetics. The circulatory model is based on TTD on inverse of Laplace transform, and may be used only under linear conditions. Saturable systems cannot be defined by this method. Accommodation of heterogeneous enzyme or transporter distribution to the circulatory model within an organ has not been tried.

Fractal models are rarely employed, but have definite usefulness in terms of describing distribution phenomena and kinetics/dynamics. Homogeneity is a presupposition typically considered in compartmental modeling, but is a departure of reality. However, the physiological implications of the fractal concepts are serious since fractal structures and processes are ubiquitous in living things, eg, the lung, the vascular system, and the distribution of blood flow through the blood vessels. Accordingly, fractal models are used when classical kinetics have been found to be unsatisfactory under dimensional constraints, eg, phase boundaries, understirred media or membrane reactions. When homogeneity cannot be applied to the structure of the organ, or when non-Fickian diffusion occurs, then fractal kinetics is more appropriate. Fractal models are plausible explanations for deviation from MM kinetics, and time-dependent coefficients derived from fractal considerations may be used to describe the nonlinear phenomenon. Overall, fractal models provide the basis for the incorporation of various heterogeneous approaches to systems where the homogeneous approaches are not sufficient to describe the system.

These advanced models are intrinsically very different. The easiest to consider in terms of mass balanced equations is the PBPK model and their heterogeneous counterparts. For circulatory models, vascular mixing may be attributed to mechanical dispersion in the microcirculatory network and result in appropriate transit time distribution. The concepts derived from fractal geometry and fractal kinetics can be used to achieve a more realistic modeling of the complex and the kinetically heterogeneous phenomena. There remains to be a lot more to be learned about these advanced models.

References

1. Nestorov I. Whole-body physiologically based pharmacokinetic models. *Expert Opin Drug Metab Toxicol*. 2007;3:235-249.

2. Rowland M, Benet LZ, Graham GG. Clearance concepts in pharmacokinetics. *J Pharmacokinet Biopharm*. 1973;1:123-136.

3. Pang KS, Rowland M. Hepatic clearance of drugs. I. Theoretical considerations of a "well-stirred" model and a "parallel tube" model. Influence of hepatic blood flow, plasma and blood cells binding, and the hepatocellular enzymatic activity on hepatic drug clearance. *J Pharmacokinet Biopharm*. 1977;5:625-653.

4. Pang KS, Chiba M. Metabolism: Scaling up from in vitro to organ and whole body. In: Welling PG, Balant LP, eds. *Handbook of Experimental Pharmacology.* Stuttgart, Germany: Springer-Verlag; 1994:101-187.

5. Liu L, Pang KS. An integrated approach to model hepatic drug clearance. *Eur J Pharm Sci*. 2006;29:215-230.

6. Liu L, Pang KS. The roles of transporters and enzymes in hepatic drug processing. *Drug Metab Dispos*. 2004;33:1-7.

7. Pang KS, Sun H, Liu S. Interplay between transporters and enzymes. In: Morris ME, You G, eds. *Drug Transporters: Molecular Characterization and Role in Drug Disposition.* Hoboken, NJ: Wiley and Sons; 2007:709-745.

8. de Lannoy IAM, 3rd, Barker F, 3rd, Pang KS. Formed and preformed metabolite excretion clearances in liver, a metabolite formation organ: studies on enalapril and enalaprilat in the single-pass and recirculating perfused rat liver. *J Pharmacokinet Biopharm*. 1993;21:395-422.

9. Sun H, Liu L, Pang KS. Increased estrogen sulfation of estradiol 17β-D glucuronide in rat metastasis tumor livers. *J Pharmacol Exp Ther*. 2006;319:818-831.

10. Hekman P, van Ginneken CA. Kinetic modeling of the renal excretion of iodopyracet in the dog. *J Pharmacokinet Biopharm*. 1982;10:77-92.

11. Boom SP, Moons MM, Russel FG. Renal tubular transport of cimetidine in the isolated perfused kidney of the rat. *Drug Metab Dispos*. 1994;22:148-153.

12. de Lannoy IAM, Hirayama H, Pang KS. A physiological model for renal drug metabolism: enalapril esterolysis to enalaprilat in the isolated perfused rat kidney. *J Pharmacokinet Biopharm*. 1990;18:561-587.

13. Doherty M, Pang KS. Route dependent metabolism of morphine in the vascularly perfused rat intestine preparation. *Pharm Res*. 2000;17:291-297.

14. Cong D, Doherty M, Pang KS. A new physiologically-based segregated flow model to explain route-intestinal metabolism. *Drug Metab Dispos*. 2000;28:224-235.

15. Benowitz N, Forsyth FP, Melmon KL, et al. Lidocaine disposition kinetics in monkey and man. I. Prediction by a perfusion model. *Clin Pharmacol Ther*. 1974;16:87-98.

16. Jarnberg J, Johanson G. Physiologically based modeling of 1,2,4-trimethylbenzene inhalation toxicokinetics. *Toxicol Appl Pharmacol*. 1999;155:203-214.

17. Klaassen CD, Slitt AL. Regulation of hepatic transporters by xenobiotic receptors. *Curr Drug Metab*. 2005;6:309-328.

18. Tirona RG, Kim RB. Nuclear receptor and drug disposition gene regulation. *J Pharm Sci*. 2005;94:1169-1186.

19. Eloranta JJ, Kullak-Ublick GA. Coordinate transcriptional regulation of bile acid homeostasis and drug metabolism. *Arch Biochem Biophys*. 2005;433:397-412.

20. Sirianni GL, Pang KS. Organ clearance concepts: new perspectives on old principles. *J Pharmacokinet Biopharm*. 1997;25:449-470.

21. Gillette JR. Factors affecting drug metabolism. *Ann N Y Acad Sci*. 1971;179:43-66.

22. Wilkinson GR, Shand DG. Commentary: a physiological approach to hepatic drug clearance. *Clin Pharmacol Ther*. 1975;18:377-390.

23. Oinonen T, Lindros KO. Zonation of hepatic cytochrome P-450 expression and regulation. *Biochem J*. 1998;55:413-421.

24. Jungermann K. Zonation of metabolism and gene expression in liver. *Histochem Cell Biol*. 1995;103:81-91.

25. Baron J, Redick HA, Guengerich FP. Immunohistochemical study on the localization and distributions of phenobarbital- and 3-methylcholanthrene-inducible cytochromes P-450 within the livers of untreated rats. *J Biol Chem*. 1981;256:5931-5937.

26. Knapp SA, Green MD, Tephly TR, et al. Immunohistochemical demonstration of isozyme- and strain-specific differences in the intralobular localizations and distributions of UDP-glucuronosyltransferases in livers of untreated rats. *Mol Pharmacol*. 1988;33:14-21.

27. Tosh D, Borthwick EB, Sharp S, et al. Heterogeneous expression of sulphotransferases in periportal and perivenous hepatocytes prepared from male and female rat liver. *Biochem Pharmacol*. 1996;51:369-374.

28. Homma H, Tada M, Nakamura T, et al. Heterogeneous zonal distributon of sulfotransferase isoenzymes in rat liver. *Arch Biochem Biophys*. 1997;339:235-241.

29. Tan E, Pang KS. Sulfation is rate-limiting in the futile cycling between estrone and estrone sulfate in enriched periportal and perivenous rat hepatocytes. *Drug Metab Dispos*. 2001;29:335-346.

30. Tirona RG, Pang KS. Bimolecular glutathione conjugation of ethacrynic acid and efflux of the glutathione adduct by periportal and perivenous rat hepatocytes. *J Pharmacol Exp Ther*. 1999;290:1230-1241.

31. Anundi IM, Kauffman FC, el-Mouelhi M, et al. Hydrolysis of organic sulfates in periportal and pericentral regions of the liver lobule: studies with 4-methylumbelliferyl sulfate in the perfused rat liver. *Mol Pharmacol*. 1986;29:599-605.

32. Stieger B, Hagenbuch B, Landmann L, et al. In situ localization of the hepatocytic Na^+/taurocholate cotransporting polypeptide in rat liver. *Gastroenterology*. 1994;107:1781-1787.

33. Abu-Zahra TN, Wolkoff AW, Kim RB, et al. Uptake of enalapril and expression of organic anion transporting polypeptide 1 in zonal, isolated rat hepatocytes. *Drug Metab Dispos*. 2000;28:801-806.

34. Liu L, Mak E, Tirona RG, et al. Vascular binding, blood flow, transporter, and enzyme interactions on the processing of digoxin in rat liver. *J Pharmacol Exp Ther*. 2005;315:433-448.

35. Reichel C, Gao B, van Montfoort J, et al. Localizatoin and function of the organic anion-transporting polypeptide Oatp2 in rat liver. *Gastroenterology*. 1999;117:688-695.

36. Cattori V, van Montfoort JE, Stieger B, et al. Localization of organic anion transporting polypeptide 4 (Oatp4) in rat liver and comparison of its substrate specificity with Oatp1, Oatp2 and Oatp3. *Pflugers Arch*. 2001;443:188-195.

37. Meyer-Wentrup F, Karbach U, Gorboulev V, et al. Membrane localization of the electrogeneic cation transporter rOCT1 in rat liver. *Biochem Biophys Res Commun*. 1998;248:673-678.

38. Gerloff T, Stieger B, Hangenbuch B, et al. The sister of P-glycoprotein represents the canalicular bile salt export pump of mammalian liver. *J Biol Chem*. 1998;273:10046-10050.

39. Donner MG, Warskulat U, Saha N, Häussinger D. Enhanced expression of basolateral multidrug resistance protein isoforms Mrp3 and Mrp5 in rat liver by LPS. *Biol Chem*. 2004;385:331-339.

40. Rappaport AM. The structural and functional unit in the human liver (liver acinus). *Anat Rec*. 1958;130:673-689.

41. Abu-Zahra TN, Pang KS. Effect of zonal transport and metabolism on hepatic removal: enalapril hydrolysis in zonal, isolated rat hepatocytes in vitro and correlation with perfusion data. *Drug Metab Dispos*. 2000;28:807-813.

42. Tirona R, Pang KS. Sequestered endoplasmic reticulum space for sequential metabolism of salicylamide: coupling of hydroxylation and glucuronidation. *Drug Metab Dispos*. 1996;24:821-833.

43. Xu X, Tang BK, Pang KS. Sequential metabolism of salicylamide exclusively to gentisamide-5-glucuronide and not gentisamide sulfate conjugates in single pass *in situ* perfused rat liver. *J Pharmacol Exp Ther*. 1990;253:963-973.

44. Doherty M, Poon K, Tsang C, et al. Transport is not rate-limiting in morphine glucuronidation in the single pass perfused rat liver preparation. *J Pharmacol Exp Ther*. 2006;317:890-900.

45. Tan E, Lu T, Pang KS. Futile cycling of estrone sulfate and estrone in the recirculating, perfused rat liver. *J Pharmacol Exp Ther*. 2001;297:423-436.

46. Pang KS. Modeling of intestinal drug absorption: roles of transporters and metabolic enzymes (Gillette Review Series). *Drug Metab Dispos*. 2003;31:1507-1519.

47. Paine MF, Shen DD, Kunze KL, et al. First-pass metabolism of midazolam by the human intestine. *Clin Pharmacol Ther*. 1996;60:14-24.

48. Paine MF, Khalighi M, Fisher JM, et al. Characterization of interintestinal and intraintestinal variations in human CYP3A-dependent metabolism. *J Pharmacol Exp Ther*. 1997;283:1552-1562.

49. Li LY, Amidon GL, Kim JS, et al. Intestinal metabolism promotes regional differences in apical uptake of indinavir: coupled effect of P-glycoprotein and cytochrome P450 3A on indinavir membrane permeability. *J Pharmacol Exp Ther*. 2002;301:586-593.

50. Koster AS, Frankhuijzen-Sierevogel AC, Noordhoek J. Glucuronidation of morphine and six β2-sympathominetics in isolated rat intestinal epithelial cells. *Drug Metab Dispos*. 1985;13:232-237.

51. Schwarz LR, Schwenk M. Sulfation in isolated enterocytes of guinea pig: dependence of inorganic sulfate. *Biochem Pharmacol*. 1984;33:3353-3356.

52. Pinkus LM, Ketley JN, Jakoby WB. The glutathione S-transferases as a possible detoxification system of rat intestinal epithelium. *Biochem Pharmacol*. 1977;26:2359-2363.

53. Huijghebaert SM, Sim SM, Back DJ, et al. Distribution of estrone sulfatase activity in the intestine of germfree and conventional rats. *J Steroid Biochem*. 1984;20:1175-1179.

54. Fei YJ, Kanai Y, Nussberger S, et al. Expression cloning of a mammalian proton-coupled oligopeptide transporter. *Nature*. 1994;368:563-566.

55. Wong MH, Oelkers P, Craddock AL, et al. Expression cloning and characterization of the hamster ileal sodium-dependent bile acid transporter. *J Biol Chem*. 1994;269:1340-1347.

56. Shneider BL, Dawson PA, Christie DM, et al. Cloning and molecular characterization of the ontogeny of a rat ileal sodium-dependent bile acid transporter. *J Clin Invest*. 1995;95:745-754.

57. Cong D, Fong AKY, Lee R, et al. Absorption of benzoic acid (BA) by segmental regions of the in situ perfused rat small intestine. *Drug Metab Dispos*. 2001;29:1539-1547.

58. Chen X, Pang KS. The effects of 1α,25-dihydroxyvitamin D_3 on transporters and enzymes associated with bile acid homeostasis in rat liver [abstract]. *AAPSJ*. 2005;S2:.

59. Liu S, Tam D, Chen X, Pang KS. An unstirred water layer and P-glycoprotein barring digoxin absorption by the perfused rat small intestine preparation: Induction studies with and without pregnenolone 16α-carbonitrile (PCN) induction. *Drug Metab Dispos*. 2006;34:1468-1479.

60. Mottino AD, Hoffman T, Jennes L, et al. Expression and localization of multidrug resistant protein mrp2 in rat small intestine. *J Pharmacol Exp Ther*. 2000;293:717-723.

61. Gotoh Y, Suzuki H, Kinoshita S, et al. Involvement of an organic anion transporter (canalicular multispecific organic anion transporter/ multidrug resistance-associated protein 2) in gastrointestinal secretion of glutathione conjugates in rats. *J Pharmacol Exp Ther*. 2000;292:433-439.

62. Rost D, Mahner S, Sugiyama Y, et al. Expression and localization of the multidrug resistance-associated protein 3 in rat small and large intestine. *Am J Physiol*. 2002;282:G720-G726.

63. Tam D, Tirona RG, Pang KS. Segmental intestinal transporters and metabolic enzymes on intestinal drug absorption. *Drug Metab Dispos*. 2003;31:373-383.

64. Matsubara T, Kim HJ, Shimada M, et al. Isolation and characterization of a new major intestineal CYP3A form, CYP3A62, in the rat. *J Pharmacol Exp Ther*. 2004;309:1282-1290.

65. Cutler DJ. A linear recirculation model for drug disposition. *J Pharmacokinet Biopharm*. 1979;7:101-116.

66. Weiss M, Förster W. Pharmacokinetic model based on circulatory transport. *Eur J Clin Pharmacol*. 1979;16:287-293.

67. Weiss M. Pharmacokinetics in organs and the intact body: model validation and reduction. *Eur J Pharm Sci*. 1999;7:119-127.

68. Krejcie TC, Avram MJ. What determines anesthetic induction dose, It's the front-end kinetics, doctor! *Anesth Analg*. 1999;89:541-544.

69. Upton RN, Ludbrook GL, Grant C, Martinez AM. Cardiac output is a determinant of the initial concentrations of propofol after short-infusion administration. *Anesth Analg*. 1999;89:545-552.

70. Krejcie TC, Avram MJ, Gentry WB, et al. A recirculatory model of the pulmonary uptake and pharmacokinetics of lidocaine based on analysis of arterial and mixed venous data from dogs. *J Pharmacokinet Biopharm*. 1997;25:169-190.

71. Krejcie TC, Wang Z, Avram MJ. Drug-induced hemodynamic perturbations alter the disposition of markers of blood volume, extracellular fluid, and total body water. *J Pharmacol Exp Ther*. 2001;296:922-930.

72. Avram MJ, Krejcie TC, Henthorn TK. The concordance of early antipyrine and thiopental distribution kinetics. *J Pharmacol Exp Ther*. 2002;302:594-600.

73. Krejcie TC, Henthorn TK, Gentry WB, et al. Modifications of blood volume alter the disposition of markers of blood volume, extracellular fluid, and total body water. *J Pharmacol Exp Ther*. 1999;291:1308-1316.

74. Kuipers JA, Boer F, Olofsen E, et al. Recirculatory pharmacokinetics and pharmacodynamics of rocuronium in patients: the influence of cardiac output. *Anesthesiology*. 2001;94:47-55.

75. Upton RN, Ludbrook GL. A physiologically based, recirculatory model of the kinetics and dynamics of propofol in man. *Anesthesiology*. 2005;103:344-352.

76. Upton RN, Grant C, Martinez AM, et al. Recirculatory model of fentanyl disposition with the brain as the target organ. *Br J Anaesth*. 2004;93:687-697.

77. Weiss M. Errors in clearance estimation after bolus injection and arterial sampling: non-existence of a central compartment. *J Pharmacokinet Biopharm*. 1997;25:255-260.

78. Weiss M, Roberts MS. Tissue distribution kinetics as determinant of transit time dispersion of drugs in organs: application of a stochastic model to the rat hindlimb. *J Pharmacokinet Biopharm*. 1996;24:173-196.

79. Upton RN. The two-compartment recirculatory pharmacokinetic model—an introduction to recirculatory pharmacokinetic concepts. *Br J Anaesth*. 2004;92:475-484.

80. Weiss M, Pang KS. The dynamics of drug distribution. I. Role of the second and third curve moment. *J Pharmacokinet Biopharm*. 1992;20:253-278.

81. Weiss M. A note on the role of generalized inverse Gaussian distributions of circulatory transit times in pharmacokinetics. *J Math Biol*. 1984;20:95-102.

82. Weiss M, Krejcie TC, Avram MJ. Transit time dispersion in the pulmonary and systemic circulation: effects of cardiac output and solute diffusivity. *Am J Physiol*. 2006;291:H861-H870.

83. Roberts MS, Anissimov YG, Weiss M. Commentary: Using the convection-dispersion model and transit time density functions in the

analysis of organ distribution kinetics. *J Pharm Sci*. 2000;89:1579-1586.

84. Oliver RE, Jones AF, Rowland M. A whole-body physiologically based pharmacokinetic model incorporating dispersion concepts: short and long time characteristics. *J Pharmacokinet Pharmacodyn*. 2001;28:27-55.

85. Karalis V, Dokoumetzidis A, Macheras P. A physiologically based approach for the estimation of recirculatory parameters. *J Pharmacol Exp Ther*. 2003;308:198-205.

86. Weiss M, Hübner GH, Hübner IG, Teichmann W. Effects of cardiac output on disposition kinetics of sorbitol: recirculatory modelling. *Br J Clin Pharmacol*. 1996;41:261-268.

87. Weiss M, Krejcie TC, Avram MJ. Circulatory transport and capillary-tissue exchange as determinants of the distribution kinetics of inulin and antipyrine in dog. *J Pharm Sci*. 2007;96:913-926.

88. Tabata K, Yamaoka K, Fukuyama T, Nakagawa T. Evaluation of intestinal absorption into the portal system in enterohepatic circulation by measuring the difference in portal-venous blood concentrations of diclofenac. *Pharm Res*. 1995;12:880-883.

89. Weiss M, Roelsgaard K, Bender D, Keiding S. Determinants of [^{13}N]ammonia kinetics in hepatic PET experiments: A minimal recirculatory model. *Eur J Nucl Med*. 2002;29:1648-1656.

90. Ben-Avraham D, Havlin S. *Diffusion and Reactions in Fractals and Disordered Systems.* New York, NY: Cambridge University Press; 2000.

91. Bassingthwaighte JB, Liebovitch LS, West BJ. *Fractal Physiology.* New York, NY: Oxford University Press; 1994.

92. Kopelman R. Fractal reaction kinetics. *Science*. 1988;241:1620-1626.

93. Macheras P, Iliadis A. *Modeling in Biopharmaceutics, Pharmacokinetics and Pharmacodynamics: Homogeneous and Heterogeneous Approaches.* New York, NY: Springer; 2006.

94. Dokoumetzidis A, Karalis V, Iliadis A, et al. The heterogeneous course of drug transit through the body. *Trends Pharmacol Sci*. 2004;25:140-146.

95. Nittmann J, Daccord G, Stanley H. Fractal growth of viscous fingers –quantitative characterization of a fluid instability phenomenon. *Nature*. 1985;314:141-144.

96. VanDamme H. *Flow and interfacial instabilities in Newtonian and colloidal fluids (or the birth, life and death of a fractal), The Fractal Approach to Heterogeneous Chemistry.* Chichester, UK: Wiley; 1989.

97. Bhaskar K, Garik P, Turner B, et al. Viscous fingering of HCl through gastric mucin. *Nature*. 1992;360:458-461.

98. Holm L, Flemstrom G. Microscopy of acid transport at the gastric surface in vivo. *J Intern Med Suppl*. 1990;732:91-95.

99. Macheras P, Argyrakis P. Gastrointestinal drug absorption: is it time to consider heterogeneity as well as homogeneity? *Pharm Res*. 1997;14:842-847.

100. Caroli-Bosc F, Iliadis A, Salmon L, et al. Ursodeoxycholic acid modulates cyclosporin A oral absorption in liver transplant recipients. *Fundam Clin Pharmacol*. 2000;14:601-609.

101. Higaki K, Yamashita S, Amidon G. Time-dependent oral absorption models. *J Pharmacokinet Pharmacodynam*. 2001;28:109-128.

102. Kalampokis A, Argyrakis P, Macheras P. Heterogeneous tube model for the study of small intestinal transit flow. *Pharm Res*. 1999;16:87-91.

103. Kalampokis A, Argyrakis P, Macheras P. A heterogeneous tube model of intestinal drug absorption based on probabilistic concepts. *Pharm Res*. 1999;16:1764-1769.

104. Wang Z, Zhenya H, Chen J. Chaotic behavior of gastric migrating myoelectrical complex. *Biomed Engr*. 2004;51:1401-1406.

105. Weibull W. A statistical distribution of wide applicability. *J Appl Mech*. 1951;18:293-297.

106. Macheras P, Dokoumetzidis A. On the heterogeneity of drug dissolution and release. *Pharm Res*. 2000;17:108-112.

107. Lansky P, Weiss M. Does the dose-solubility ratio affect the mean dissolution time of drugs? *Pharm Res*. 1999;16:1470-1476.

108. Lansky P, Weiss M. Modeling heterogeneity of properties and random effects in drug dissolution. *Pharm Res*. 2001;18:1061-1067.

109. Lansky P, Weiss M. Classification of dissolution profiles in terms of fractional dissolution rate and a novel measure of heterogeneity. *J Pharm Sci*. 2003;92:1632-1647.

110. Dokoumetzidis A, Macheras P. A population growth model of dissolution. *Pharm Res*. 1997;14:1122-1126.

111. Valsami G, Dokoumetzidis A, Macheras P. Modeling of supersaturated dissolution data. *Int J Pharm*. 1999;181:153-157.

112. Bunde A, Havlin S, Nossal R, Stanley HE, Weiss GH. On controlled diffusion-limited drug release from a leaky matrix. *J Chem Phys*. 1985;83:5909-5913.

113. Kosmidis K, Argyrakis P, Macheras P. A reappraisal of drug release laws using Monte Carlo simulations: the prevalence of the Weibull function. *Pharm Res*. 2003;20:988-995.

114. Kosmidis K, Argyrakis P, Macheras P. Fractal kinetics in drug release from finite fractal matrices. *J Chem Phys*. 2003;119:6373-6377.

115. Villalobos R, Vidales AM, Cordero S, Quintanar D, Domnguez A. Monte Carlo simulation of diffusion-limited drug release from finite fractal matrices. *J Sol-Gel Sci Technol*. 2006;37:195-199.

116. Villalobos R, Ganem A, Cordero S, et al. Effect of the drug-excipient ratio in matrix-type-controlled realease systems: computer simulation study. *Drug Dev Ind Pharm*. 2005;31:535-543.

117. Haddish-Berhane N, Nyquist C, Haghighi K, et al. A multi-scale stochastic drug release model for polymer-coated targeted drug delivery systems. *J Control Release*. 2006;110:314-322.

118. Barat A, Ruskin HJ, Crane M. Probabilistic models for drug dissolution. Part 1. Review of Monte Carlo and stochastic cellular automata approaches. *Simul Model Pract Th*. 2006;14:834-856.

119. Barat A, Ruskin HJ, Crane M. Probabilistic methods for drug dissolution. Part 2. Modelling a soluble binary drug delivery system dissolving in vitro. *Simul Model Pract Th*. 2006;14:857-873.

120. Papadopoulou V, Kosmidis K, Vlachou M, Macheras P. On the use of the Weibull function for the discernment of drug release mechanisms. *Int J Pharm*. 2006;309:44-50.

121. West G, Brown J, Enquist B. A general model for the origin of allometric scaling laws in biology. *Science*. 1997;276:122-126.

122. West GB, Brown J, Enquist B. The fourth dimension of life: fractal geometry and allometric scaling of organisms. *Science*. 1999;284:1677-1679.

123. Karalis V, Claret L, Iliadis A, Macheras P. Fractal volume of drug distribution: it scales proportionally to body mass. *Pharm Res*. 2001;18:1056-1060.

124. Laffon E, Suarez K, Berthoumieu Y, Ducassou D, Marthan R. Normalization in quantitative [^{18}F]FDG PET imaging: the "body surface area" may be a volume. *Phys Med Biol*. 2006;51:N47-N50.

125. Karalis V, Macheras P. Drug disposition viewed in terms of the fractal volume of distribution. *Pharm Res*. 2002;19:697-704.

126. Karalis V, Tsantili A, Macheras P. Multivariate statistics of disposition pharmacokinetic parameters for structurally unrelated drugs used in therapeutics. *Pharm Res*. 2002;19:1829-1836.

127. Karalis V, Tsantili A, Macheras P. Quantitative structure pharmacokinetic relationships for disposition parameters of cephalosporins. *Eur J Pharm Sci*. 2003;20:115-123.

128. Dokoumetzidis A, Macheras P. A tube model for transport and dispersion in the circulatory system based on the vascular fractal tree. *Ann Biomed Eng*. 2003;31:284-293.

129. Claret L, Iliadis A, Macheras P. A stochastic model describes the heterogeneous pharmacokinetics of cyclosporin. *J Pharmacokinet Pharmacodyn*. 2001;28:445-463.

130. Rescigno A. The rise and fall of compartmental analysis. *Pharmacol Res*. 2001;44:337-342.

131. Wise ME, Borsboom JM. Two exceptional sets of physiological clearance curves and their mathematical form: test cases? *Bull Math Biol*. 1989;51:579-596.

132. Matis JH, Wehrly TE. A general approach to non-Markovian compartmental models. *J Pharmacokinet Biopharm*. 1998;26:437-456.

133. Weiss GH, Goans RE, Gitterman M, Abrams SA, Vieira NE, Yergey AL. A non-Markovian model for calcium kinetics in the body. *J Pharmacokinet Biopharm*. 1994;22:367-379.

134. Macheras P. A fractal approach to heterogeneous drug distribution: calcium pharmacokinetics. *Pharm Res*. 1996;13:663-670.

135. Weiss M. The anomalous pharmacokinetics of amiodarone explained by nonexponential tissue trapping. *J Pharmacokinet Biopharm*. 1999;27:383-396.

136. López-Quintela M, Casado J. Revision of the methodology in enzyme kinetics: a fractal approach. *J Theor Biol*. 1989;139:129-139.

137. Savageau MA. Michaelis-Menten mechanism reconsidered: implications of fractal kinetics. *J Theor Biol*. 1995;176:115-124.

138. Savageau MA. Development of fractal kinetic theory for enzyme-catalysed reactions and implications for the design of biochemical pathways. *Biosystems*. 1998;47:9-36.

139. Berry H. Monte Carlo simulations of enzyme reactions in two dimensions: fractal kinetics and spatial segregation. *Biophys J*. 2002;83:1891-1901.

140. Fuite J, Marsh R, Tuszynski J. Fractal pharmacokinetics of the drug mibefradil in the liver. *Phys Rev E*. 2002;66:21904.

141. Kosmidis K, Karalis V, Argyrakis P, et al. Michaelis Menten kinetics under spatially constrained conditions: application to mibefradil pharmacokinetics. *Biophys J*. 2004;87:1498-1506.

142. Marsh R, Tuszynski JA. Fractal Michaelis-Menten kinetics under steady state conditions: application to mibefradil. *Pharm Res*. 2006;23:2760-2767.

143. Chelminiak P, Dixon JM, Tuszynski JA, et al. Application of a random network with a variable geometry of links to the kinetics of drug elimination in healthy and diseased livers. *Phys Rev E*. 2006;5:51912.